Visualization of Hydrogen Bonding and Associated Chirality in Methanol Hexamers

Timothy J. Lawton,[1] Javier Carrasco,[2] Ashleigh E. Baber,[1] Angelos Michaelides,[3] and E. Charles H. Sykes[1,*]

[1]*Department of Chemistry, Tufts University, Medford, Massachusetts 02155-5813, USA*

[2]*Instituto de Catálisis y Petroleoquímica, CSIC, Marie Curie 2, E-28049 Madrid, Spain*

[3]*Thomas Young Centre, London Centre for Nanotechnology and Department of Chemistry, University College London, London WC1E 6BT, United Kingdom*

(Received 4 August 2011; revised manuscript received 13 October 2011; published 16 December 2011)

Using a combination of scanning tunneling microscopy (STM) and density functional theory the hydrogen bond directionality and associated chirality of enantiopure clusters is visualized and controlled. This is demonstrated with methanol hexamers adsorbed on Au(111), which depending on their chirality, adopt two distinct molecular footprints on the surface. Controlled STM tip manipulations were used to interconvert the chirality of entire clusters and to break up metastable chain structures into hexamers.

DOI: 10.1103/PhysRevLett.107.256101 PACS numbers: 68.43.Hn, 68.37.Ef, 68.43.Bc, 68.47.De

Hydrogen (H) bonded networks are ubiquitous in nature and crucial to the integrity of many materials. H bonding is also of increasing importance to nanoscience, being key to the patterning of surfaces with ordered molecular overlayers [1]. H bonding between small molecules can lead to remarkably complex structures [2–7] and recently self-assembled systems built from larger molecules with multiple H bonds per molecule have exhibited significant stability >550 K [8]. One intriguing aspect of H bonded networks is that their structure implies they must have directionality and hence, in nonlinear systems, an associated chirality [2,3,6,7]. At solid surfaces the chirality of 2D H bonded networks has been extensively examined in recent years, motivated by the relevance to chemical synthesis and chiral heterogeneous catalysis [9]. For example, it is well known that adsorption of chiral molecules on catalytic surfaces can render them with enantioselective adsorption and reactivity properties [10]. Less appreciated is that achiral molecules can become chiral upon adsorption [2,3,7,11–13], or that an achiral functionality within the molecule can take on a chiral footprint [14] and that this surface-induced chirality may lead to important diastereomeric effects in the interaction with other chiral species. A key early study revealed that adsorption-induced chirality, coupled with hydrogen bonding between adjacent molecules, led to clear mirror image superstructures with defined chirality that could even be moved across the surface intact [2,3].

Low-temperature scanning tunneling microscopy (STM), often in conjunction with density functional theory (DFT), is a powerful approach for obtaining direct real-space access to H bonding and chirality at the nanoscale [2,3,7,14–20]. A rich variety of H bonded overlayer structures has been resolved and, of these, water adlayers are perhaps the best understood. However, even with the highest resolution data for water it has not been possible to discern the directionality and detailed topology of H bonded networks, or establish if the structures have an associated chirality [16–20]. Water is challenging because the individual molecules are usually imaged as single protrusions in STM. Methanol (CH_3OH), on the other hand, has the necessary asymmetry that may enable the orientation of the molecules in the H bonded networks to be discerned. Indeed methanol represents the simplest molecule for understanding H bonded networks built of hydroxyl groups, which are one of the most common motifs in both chemical and biological systems [21–28]. As yet many aspects of the topology, including the question of proton localization or delocalization, within such O–H $\cdots$ O bonds are not fully understood and, indeed, a matter of some debate in a number of different fields [29,30].

Herein we use low-temperature STM to show that Au(111) surface-adsorbed methanol, just like water, forms stable hexamers and that the chirality of the hexamers can be imaged. DFT calculations demonstrate that this chirality arises from the directionality of the H bonded network and that clusters of different chirality have different footprints on the surface [2,3,7,14,31]. Specifically, clusters with a clockwise sequence of H bonds exhibit a clockwise rotation, and those with an anticlockwise network of H bonds an anticlockwise rotation. We further show through controlled STM tip manipulation that the chirality of the clusters can be interchanged. We anticipate that this approach will offer insight into the H bonding of other important structures including self-assembled monolayers, clusters, or micelles and the opportunity to study effects like H bond assembly, proton localization, and proton reordering [32] with an unprecedented level of detail in one of the most ubiquitous classes of H bonded network.

The low-temperature STM images (5 K) in Fig. 1 reveal that at low surface coverage (< 0.2 monolayers), methanol forms six-lobed units measuring 0.67 ± 0.06 nm between opposite maxima. This size is consistent with the rings being composed of six methanol molecules. Au(111) in its

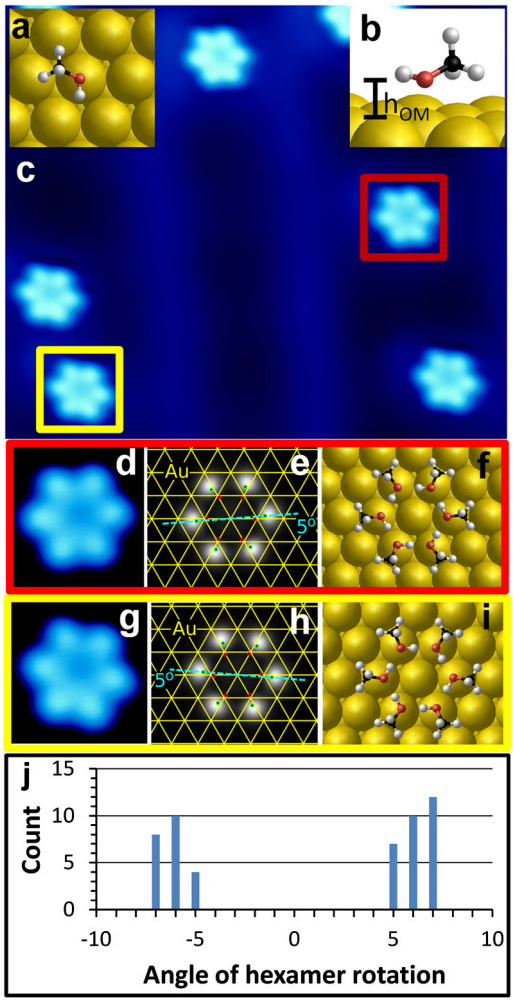

FIG. 1 (color online). (a),(b) Top and side view of the DFT predicted adsorption site of a single methanol molecule. (c) Topographic STM image of several methanol hexamers on Au(111), appearing at two discrete angles with respect to the underlying Au(111) lattice. 5 K: −0.1 V 40 pA 12 nm × 10 nm. (d),(e),(f) High resolution topographic image, simulated STM image (at 0.65 nm from the metal surface and $V = -0.1$ V) and DFT structure of a methanol hexamer with an anticlockwise O–H · · · O H bonded network. (g),(h),(i) Same data for the opposite, clockwise rotated enantiomer. STM images (d),(g) taken at 5 K: −0.1 V 40 pA 1.5 nm × 1.5 nm. (j) Experimental measure of the rotation of the hexamers with respect to the close-packed direction of the underlying Au lattice.

native $22 \times \sqrt{3}$ or herringbone reconstruction exhibits wider face-centered cubic (fcc) close-packed and narrower hexagonally close-packed (hcp) zones separated by soliton walls which appear as faint vertical lines in the main panel of Fig. 1. The herringbone reconstruction is unaffected by methanol adsorption from 5 K up to its desorption temperature [15]. Methanol hexamers display a preference (90:10) for binding in the fcc regions of the surface; therefore, we focus on these species and use an unreconstructed (111) fcc slab in the DFT calculations.

A close inspection of the high resolution data in Fig. 1 indicates that there are two types of hexamer on the surface that differ only in their rotation with respect to the Au(111) lattice. The two squares in Fig. 1 highlight an example of each type of hexamer. High resolution imaging of >50 species indicated that the two types of hexamer are present in equal amounts, hinting that the structures are isoenergetic. The bar graph in Fig. 1 indicates that the hexamers are rotated on average ±6° from the close-packed direction. These results lead us to postulate that the hexamer rotation arises from the directionality of the H bonded network and to explore methanol adsorption with DFT.

The DFT calculations were performed with the VASP code [33,34] and the Perdew, Burke, Ernzerhof (PBE) [35] and optB88–van der Waals (vdW) [36] functionals on periodic Au(111) slab models. Details of the calculations are found in the Supplemental Material [37]. They reveal that the most stable structure for a single adsorbed methanol has the O atom near atop with the O-H bond nearly parallel to the surface and with the methyl group in a top-hollow-bridge configuration [Figs. 1(a) and 1(b)]. This basic structure agrees with previous calculations for methanol on Au(111) [22,38]. Importantly, the DFT structure for individual methanol molecules on Au(111) reveals that the adsorbed molecules are themselves chiral. While methanol in the gas phase is achiral, the two lone pairs on the oxygen atom are prochiral. Preferential binding of one of these lone pairs to the Au surface leads to four inequivalent groups (lone pair, H, CH_3, and Au) around the central oxygen with approximately tetrahedral geometry and hence the formation of nonsuperimposable mirror image structures [39]. The methanol molecule shown in Fig. 1(a) is therefore of *R* chirality as defined by the Cahn-Ingold-Prelog rules.

For the methanol hexamers, many different structures and adsorption sites were considered in our calculations. In the most stable hexamer each methanol monomer remains close to the Au atop sites with the O-H bonds remaining almost parallel to the surface. Each methanol donates and accepts just one H bond yielding a cyclic methanol hexamer, similar to the water hexamers observed before [19]. However, unlike the water hexamers, the methanol hexamers are planar and no buckling in the O atom heights is found; all six oxygen-metal distances (h_{OM}) are the same (Table I). The O-O distance in the methanol hexamers (0.268 nm) is less than the Au-Au distance (0.293 nm in our calculations) of the underlying substrate revealing that the methanol molecules have all moved towards each other and are not pinned to the precise atop sites. The internal O-O-O angles are 120° and the H bonds between each monomer are within 2° of being perfectly linear.

When viewed from above the most stable hexamers are rotated slightly with respect to the substrate. From the simulated STM images we see that it is the highest lying H atoms of the CH_3 groups that image brightest

TABLE I. Average O atom height above the surface (h_{OM}), average O-O distance between methanol molecules ($d_{O\text{-}O}$), and adsorption energies (E_{ads}), calculated with PBE and optB88-vdW. E_{ads} was calculated by subtracting the total energy of the adsorbed methanol molecules from the total energies of the relaxed bare metal slab and isolated gas phase methanol molecules. Distances are in nanometers and energies are in meV/methanol molecule.

	PBE			optB88-vdW		
	h_{OM}	d_{O-O}	E_{ads}	h_{OM}	d_{O-O}	E_{ads}
Monomer	0.276	⋯	−102	0.264	⋯	−389
Hexamer (5°)	0.304	0.268	−381	0.280	0.268	−691
Chain	0.308	0.279	−362	0.283	0.277	−681

[Figs. 1(d)–1(i)]; therefore, in the calculations the rotation angle was defined as the average rotation of the hexagon of the six highest lying H atoms with respect to the Au hexagon of the adsorption site. The potential energy surface for rotation is very flat for rotations of about 5°–10° from the surface's close-packed direction, with the most stable structure identified having a rotation angle of 5° (Fig. 1). The energy of the 0° structure was computed but found to be so unstable that the molecules moved back to their original rotated configuration. We also performed a constrained optimization with the methanol hexamer at 0° and with nonlinear internal H bonds. This calculation revealed that the 0° hexamer was ∼20 meV/methanol less stable than the most stable (rotated) hexamer. The rotation is a geometric effect, resulting from the smaller internal angle of methanol (ca. 109°) compared to the 120° hexagonal angle of the surface. The hexamers with a clockwise O–H ⋯ O–H H bonded network are rotated clockwise from the nearest surface close-packed direction and those with an anticlockwise H bonded network are rotated anticlockwise from it rendering them mirror image enantiomers of one another. Each chiral hexamer is composed of six methanol enantiomers of the same chirality and hence their assembly is enantiospecific and the chirality from the monomer units is transmitted to the rotated (and hence chiral) adsorption footprint of the hexamers [14,31]. The idea of a chiral footprint is a recent and important consideration in a molecule's enantiospecific interaction with neighbors [14] and here we show that a cluster built of homochiral units can exhibit such a footprint. A chirality can be assigned to the hexamers using *P* and *M* chirality descriptors equivalent to *R* and *S* but in the helical definition of chirality [40] in which a clockwise rotation of the hexamer from the substrate would denote *M* chirality and vice versa. Our results reveal that *S* enantiomers of surface-bound methanol form *M* hexamers and *R* enantiomers form *P* hexamers in an enantiospecific manner.

Not only are the DFT calculations helpful in resolving the precise atomic-level structure of the hexamers, but they also shed light on their stability. With the optB88-vdW functional the adsorption energy of the hexamers is about 700 meV/methanol. This is an enhancement in the adsorption energy of an isolated methanol of about 300 meV. Decomposition of the adsorption energy into methanol-methanol and methanol-metal bonding shows that the ca. 700 meV adsorption energy is split almost equally between methanol-methanol (352 meV) and methanol-Au interactions (339 meV). With PBE the total adsorption energy is only about 380 meV/methanol, implying that vdW forces (accounted for only with optB88-vdW) make a major contribution to the adsorption energy.

In areas that contained locally higher coverages of methanol, chain structures were observed such as the one shown in Fig. 2. The individual units are consistent with the size of methanol molecules and DFT optimization [panels (b) and (c)] reveals that a zigzag arrangement of near atop oxygen adsorption sites leads to an ordered chain structure which runs in the three equivalent non-close-packed (or $\sqrt{3}$) directions of the Au(111) surface. The position and spacing of the methanol units match those measured experimentally and the DFT calculations indicate that the methanol chain structures are slightly less stable than the hexamers [Table I].

In order to investigate the stability and interchange of the methanol structures we employed STM tip-induced motion. Panels (a)–(c) in Fig. 3 reveal an interesting result, namely, that the chirality of an individual methanol hexamer can be altered by voltage pulsing in its vicinity. The square in (a) indicates that its initial adsorption site is rotated 6° clockwise from the close-packed direction of the surface lattice (*M* chirality). After the first pulse the hexamer appears to be broken open and frozen in an intermediate state. A subsequent pulse reforms the hexamer and imaging reveals that it is rotated 6° anticlockwise and hence of the opposite *P* chirality [box in panel (c)]. This result in which the chirality of a whole cluster can be flipped builds on recent work which showed that the

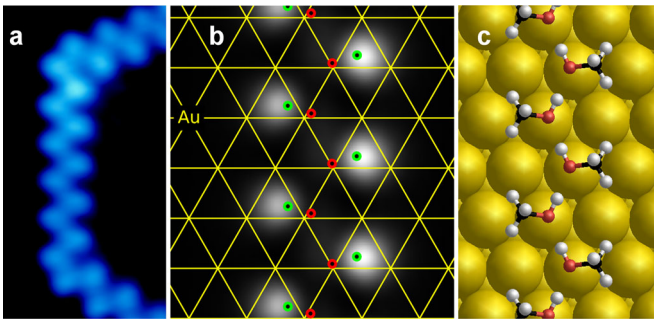

FIG. 2 (color online). (a) STM image of a section of a methanol zigzag chain that runs in three equivalent directions that correlate to the next nearest neighbor (or $\sqrt{3}$) directions of the underlying Au lattice. 5 K: −0.1 V 20 pA 2.5 nm × 4.7 nm. (b) Simulated STM image of a methanol chain (at 0.66 nm from the metal surface and $V = -0.1$ V). (c) DFT optimization showing the H bonded network within a chain.

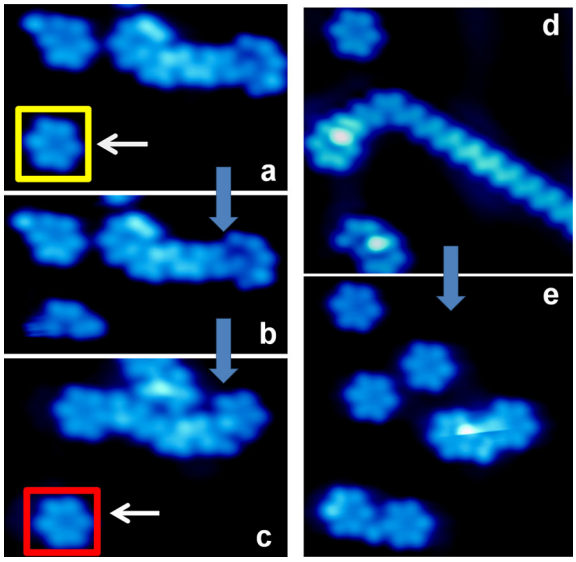

FIG. 3 (color online). STM images (a)–(c) illustrate that a clockwise rotated hexamer could be converted into the opposite enantiomer with voltage pulses (− 0.4 V). Image (b) suggests that the interconversion occurs via breakage of H bonds within the hexamer, unwrapping and reformation of the ring structure. Images (d) and (e) show the transformation of a chain structure into discrete hexamers. The methanol chain was broken apart with several voltage pulses applied in the vicinity of the chain. 5 K −0.1 V 30 pA. Images (a) 5.4 nm × 3.4 nm, (b) 5.4 nm × 2.9 nm, (c) 5.4 nm × 3.4 nm, (d) 6.4 nm × 6.3 nm, (e) 6.0 nm × 6.3 nm.

chirality of individual surface-adsorbed enantiomeric molecules could be switched via tip-induced excitation [12,13]. Figures 3(d) and 3(e) show how voltage pulses applied to the STM tip can also be used to disrupt the chain structures and that breakage of the chain results predominantly in the formation of hexamers. Our DFT calculations (Table I) indicate that the chain structures are slightly less stable than the hexamers (∼10 meV/methanol with optB88-vdW), which is consistent with the observation that the chains break into hexamers under perturbative scanning conditions. This result is supported by the fact that thermal annealing of intermediate coverages of methanol in both chain and hexamer form produced predominantly methanol hexamers.

In summary, we have used a combination of STM and DFT to show that the directionality and associated chirality of H bonded clusters can be visualized and manipulated in individual structures. Our observations of methanol hexamers with two distinct structures and different H bonding networks is evidence that even at the cryogenic temperatures of the current experiments (5 K) the protons within the H bonds are localized at individual oxygen atoms resulting in one short (covalent) and one long (H) bond between each pair of oxygens. These observations raise the possibility of interesting follow-on single molecule studies in which, for example, the asymmetry of the H bond and extent of quantum delocalization of the shared proton could be systematically explored with analogous studies on other surfaces and open up unique possibilities to make measurements of H vs D tunneling rates between adjacent oxygen atoms. One may even consider the exciting possibility of information exchange along the long MeOH chains we report via H hopping between the two equivalent structures implied by the two possible chiralities of the chain.

The authors thank the U.S. Department of Energy, the National Science Foundation, and the Camille and Henry Dreyfus Foundation for support of this work. T. J. L. acknowledges the Department of Education for support. J. C. is supported by the Spanish Ministerio de Ciencia e Innovación. A. M. is supported by the EPSRC and the European Research Council. Computational resources from the London Centre for Nanotechnology and UCL Research Computing are gratefully acknowledged. Support was also received partly via the U.K.'s HPC Materials Chemistry Consortium, which is funded by EPSRC (EP/F067496), this work made use of the facilities of HECToR.

*charles.sykes@tufts.edu

[1] J. V. Barth, Annu. Rev. Phys. Chem. **58**, 375 (2007).
[2] M. Bohringer *et al.*, Phys. Rev. Lett. **83**, 324 (1999).
[3] M. Bohringer *et al.*, Angew. Chem., Int. Ed. **38**, 821 (1999).
[4] J. Adisoejoso *et al.*, Angew. Chem., Int. Ed. **48**, 7353 (2009).
[5] J. A. Theobald *et al.*, Nature (London) **424**, 1029 (2003).
[6] R. Otero *et al.*, Angew. Chem., Int. Ed. **44**, 2270 (2005).
[7] J. Weckesser *et al.*, Phys. Rev. Lett. **87**, 096101 (2001).
[8] M. Stohr *et al.*, Angew. Chem., Int. Ed. **44**, 7394 (2005).
[9] S. M. Barlow and R. Raval, Surf. Sci. Rep. **50**, 201 (2003).
[10] T. Mallat, E. Orglmeister, and A. Baiker, Chem. Rev. **107**, 4863 (2007).
[11] A. Mugarza *et al.*, Phys. Rev. Lett. **105**, 115702 (2010).
[12] M. Parschau *et al.*, Angew. Chem., Int. Ed. **48**, 4065 (2009).
[13] V. Simic-Milosevic, J. Meyer, and K. Morgenstern, Angew. Chem., Int. Ed. **48**, 4061 (2009).
[14] A. G. Mark, M. Forster, and R. Raval, Chem. Phys. Chem. **12**, 1474 (2011).
[15] A. E. Baber, T. J. Lawton, and E. C. H. Sykes, J. Phys. Chem. C **115**, 9157 (2011).
[16] J. Carrasco *et al.*, Nature Mater. **8**, 427 (2009).
[17] J. Cerda *et al.*, Phys. Rev. Lett. **93**, 116101 (2004).
[18] H. Gawronski *et al.*, Phys. Rev. Lett. **101**, 136102 (2008).
[19] A. Michaelides and K. Morgenstern, Nature Mater. **6**, 597 (2007).
[20] T. Mitsui *et al.*, Science **297**, 1850 (2002).
[21] S. L. Boyd and R. J. Boyd, J. Chem. Theory Comput. **3**, 54 (2007).

[22] W. K. Chen *et al.*, J. Mol. Struct., Theochem **770**, 87 (2006).
[23] J. Gong *et al.*, J. Phys. Chem. C **112**, 5501 (2008).
[24] M. Haughney, M. Ferrario, and I. R. McDonald, J. Phys. Chem. **91**, 4934 (1987).
[25] S. Kashtanov *et al.*, Phys. Rev. B **71**, 104205 (2005).
[26] K. Lin *et al.*, J. Phys. Chem. B **114**, 3567 (2010).
[27] R. Ludwig, Chem. Phys. Chem. **6**, 1369 (2005).
[28] C. Panja, N. Saliba, and B. E. Koel, Surf. Sci. **395**, 248 (1998).
[29] X.-Z. Li, B. Walker, and A. Michaelides, Proc. Natl. Acad. Sci. U.S.A. **108**, 6369 (2011).
[30] J. A. Morrone and R. Car, Phys. Rev. Lett. **101**, 017801 (2008).
[31] G. Jones *et al.*, Surf. Sci. **600**, 1924 (2006).
[32] P. Liljeroth, J. Repp, and G. Meyer, Science **317**, 1203 (2007).
[33] G. Kresse and J. Furthmuller, Phys. Rev. B **54**, 11 169 (1996).
[34] G. Kresse and J. Hafner, Phys. Rev. B **47**, 558 (1993).
[35] J. P. Perdew, K. Burke, and M. Ernzerhof, Phys. Rev. Lett. **77**, 3865 (1996).
[36] J. Klimes, D. R. Bowler, and A. Michaelides, J. Phys. Condens. Matter **22**, 022201 (2010).
[37] See Supplemental Material at http://link.aps.org/supplemental/10.1103/PhysRevLett.107.256101 for additional information on theoretical and experimental methods.
[38] B. J. Xu *et al.*, J. Phys. Chem. C **115**, 3703 (2011).
[39] H. L. Tierney *et al.*, J. Phys. Chem. C **115**, 897 (2011).
[40] E. L. Eliel and S. H. Wilen, *Stereochemistry of Organic Compounds* (John Wiley & Sons, Inc., New York, 1994).